

BSU Institute
for Nuclear Problems

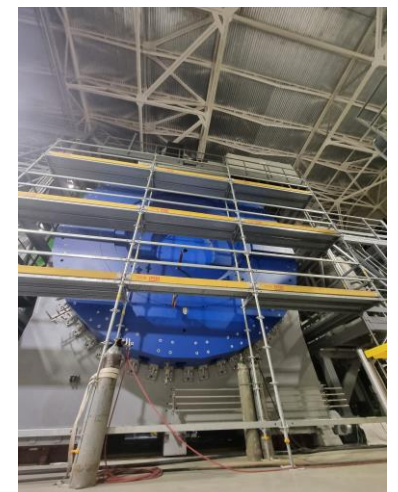
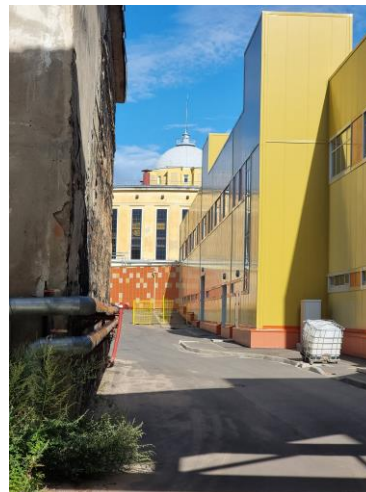
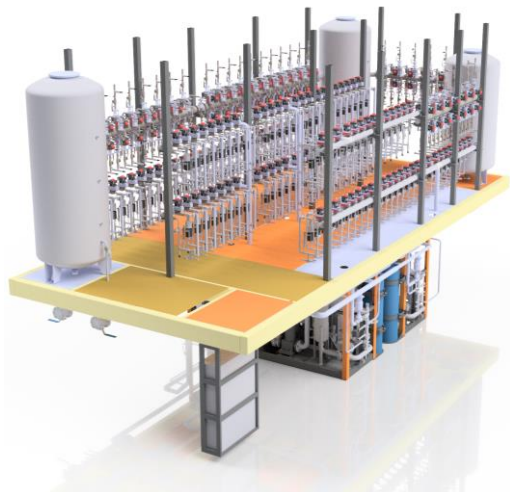


Influence of boundary thermal fluctuations on event coordinate determination in a Time-projection chamber

Alexander Fedotov¹, Ilya Zur², Yulia Shafarevich², Yaroslav Galkin²,
Aliaksei Kunts², Sergey Movchan¹

1 – LHEP JINR

2 – Research Institute for Nuclear Problems of BSU)



Nuclotron-based Ion Collider fAcility

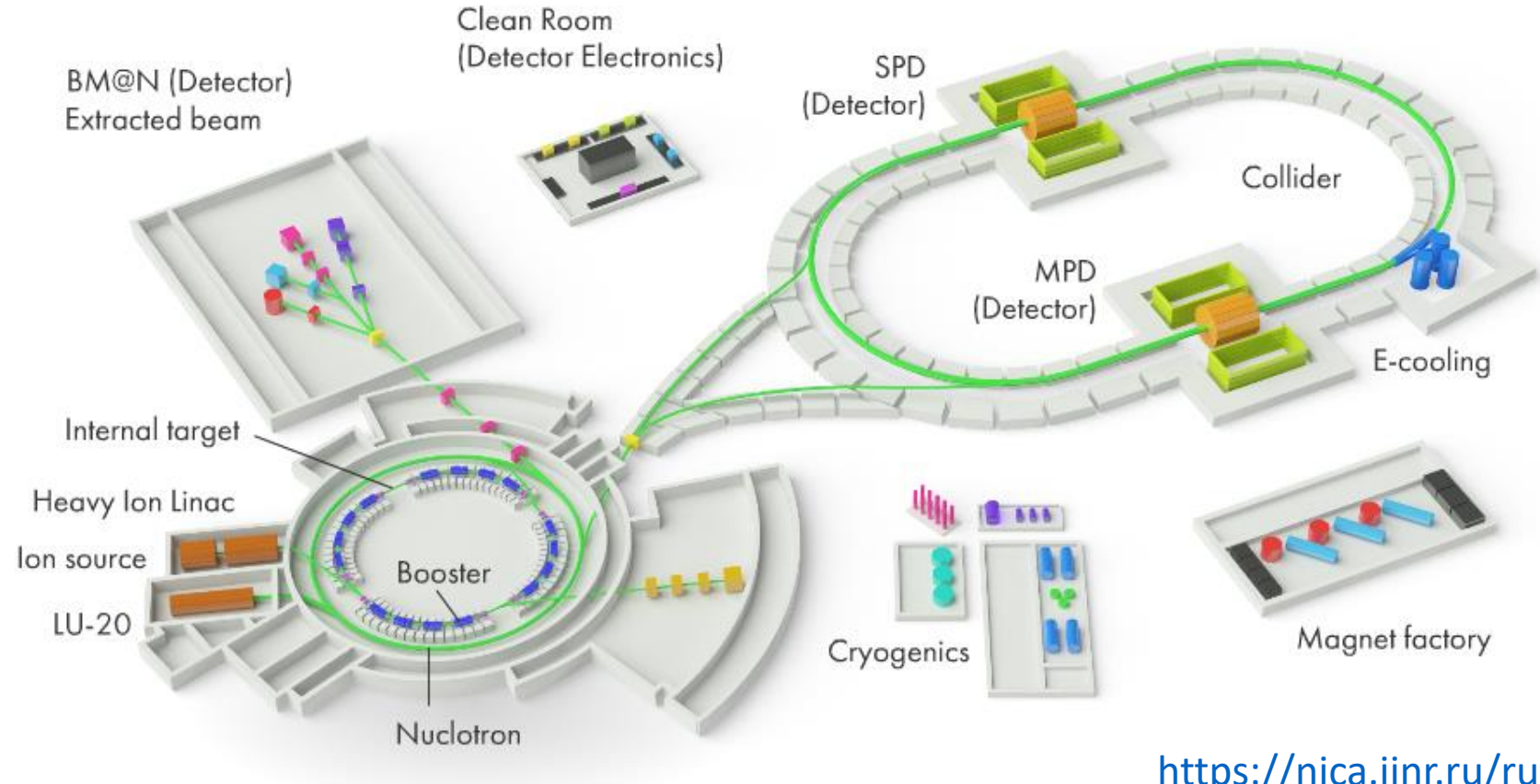
NICA – heavy-ion accelerator complex in the framework of Megascience project

NICA project objective:

Study of the phase diagram of nuclear matter

Accelerator complex:

- **Nuclotron** — basic synchrotron for ion acceleration;
- **NICA Collider** — collisions on counter-punches;
- **Multi-Purpose Detector** – the main NICA detector.



<https://nica.jinr.ru/ru/>

Energy range:
4 - 11 GeV/nucleon.

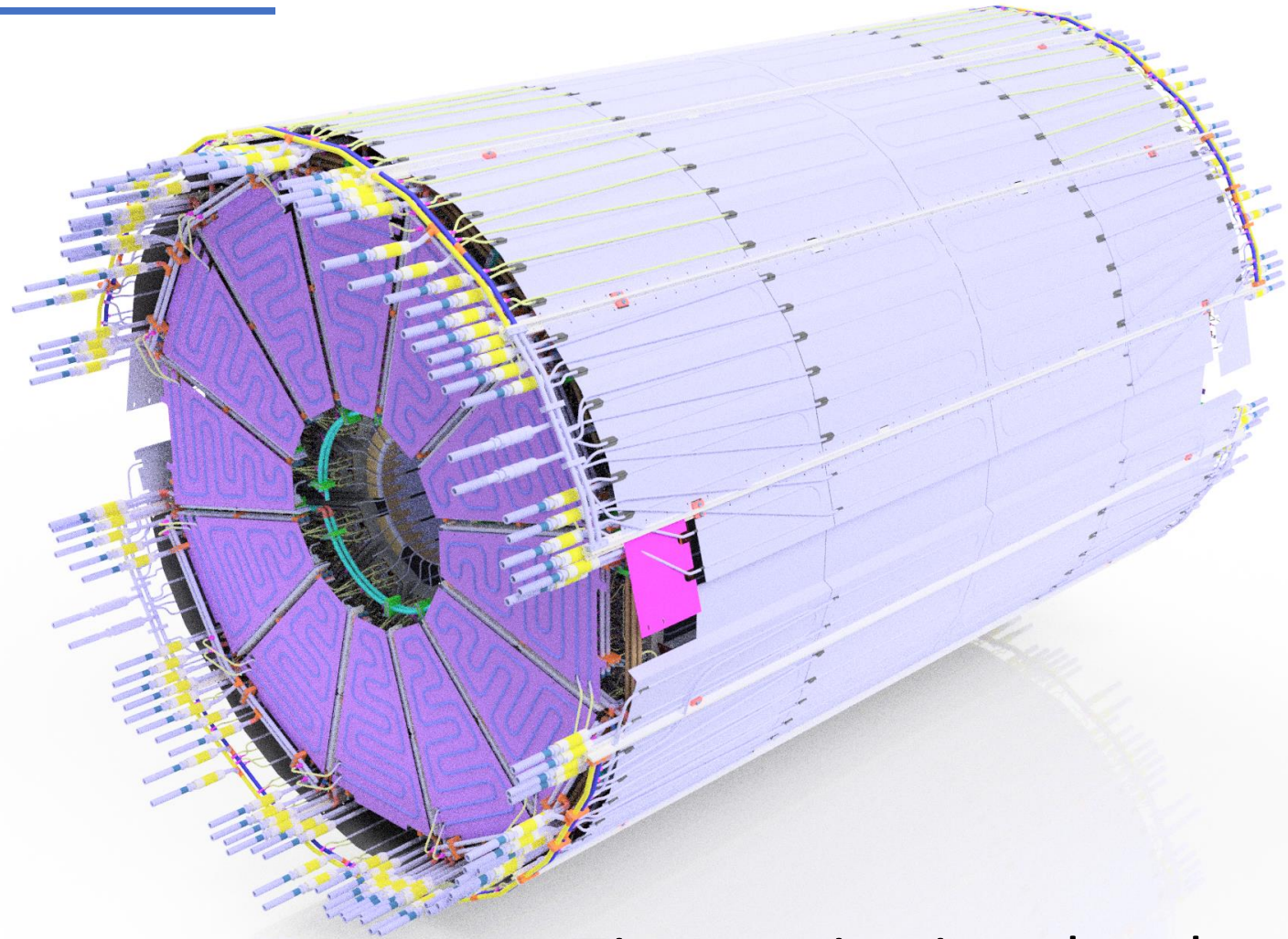
Infrastructure of the NICA Accelerator Complex

Time-projection chamber

Time-projection chamber – MPD
primary sub-detector

Principle of work:

1. A nuclear reaction product ionizes the argon-methane mixture. This process creates an electron track;
2. Electrons drift in electric field toward detectors located at both ends of the cylindrical chamber;
3. Thermal stabilization of the internal gas volume ensures constant electron drift velocity and accurate particle identification



Time-projection chamber

Goal and objectives

Goal: explore the influence of thermal stabilization on the precision of TPC

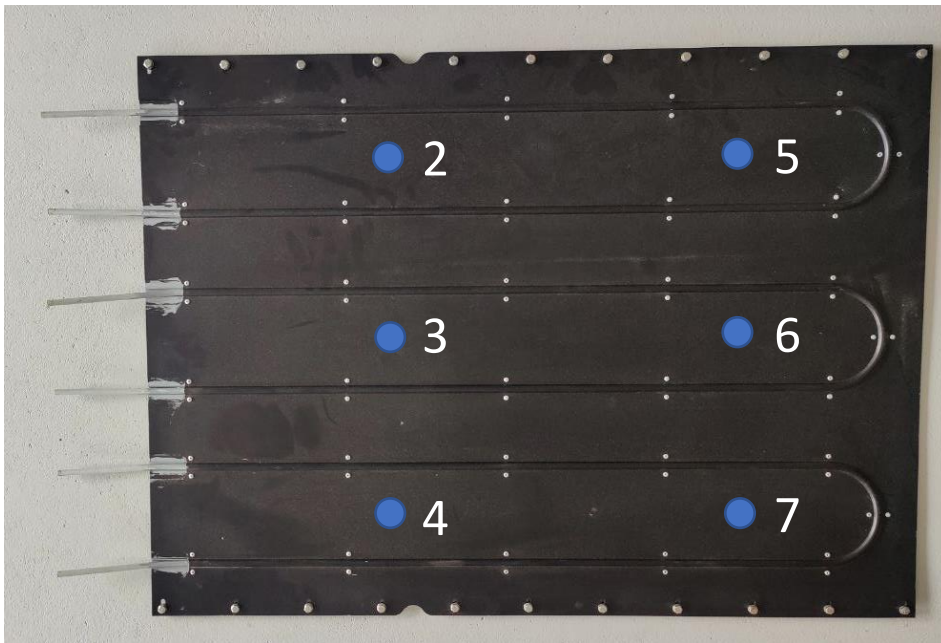
Objectives:

- Estimate the temperature inhomogeneity degree at the boundary of the working gas volume in TPC;
- Determine the influence of temperature inhomogeneity on event detection accuracy.

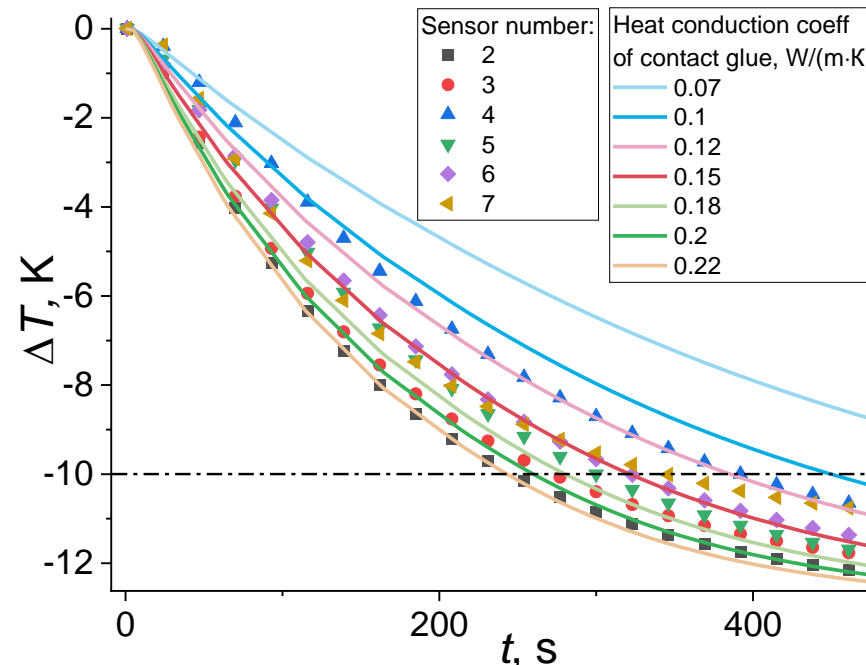
External thermal screen

External thermal screen – set of aluminum plates with water pipes bounding the working gas volume.

Experiment: the panel is placed in an insulated box and brought to equilibrium, then cold water is ‘instantaneously’ supplied $T_{water} = T_{room} - 12.6 \text{ K}$, 1 m/s



Single panel of thermal screen



Time dependence of temperature at sensor points
dots - experiment, solid lines - COMSOL reconstruction

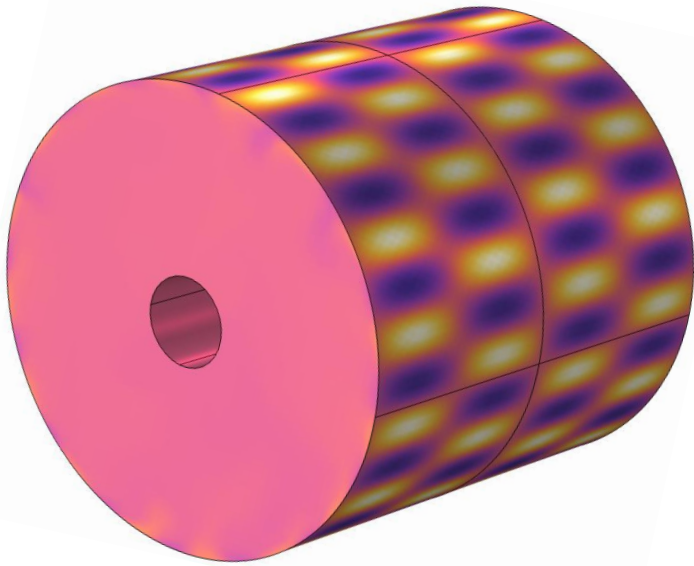
The difference in the curves slope is explained by different quality of thermal contact between the pipe and the radiator - the resistance of the adhesive layer

Inhomogeneity on the thermal screen

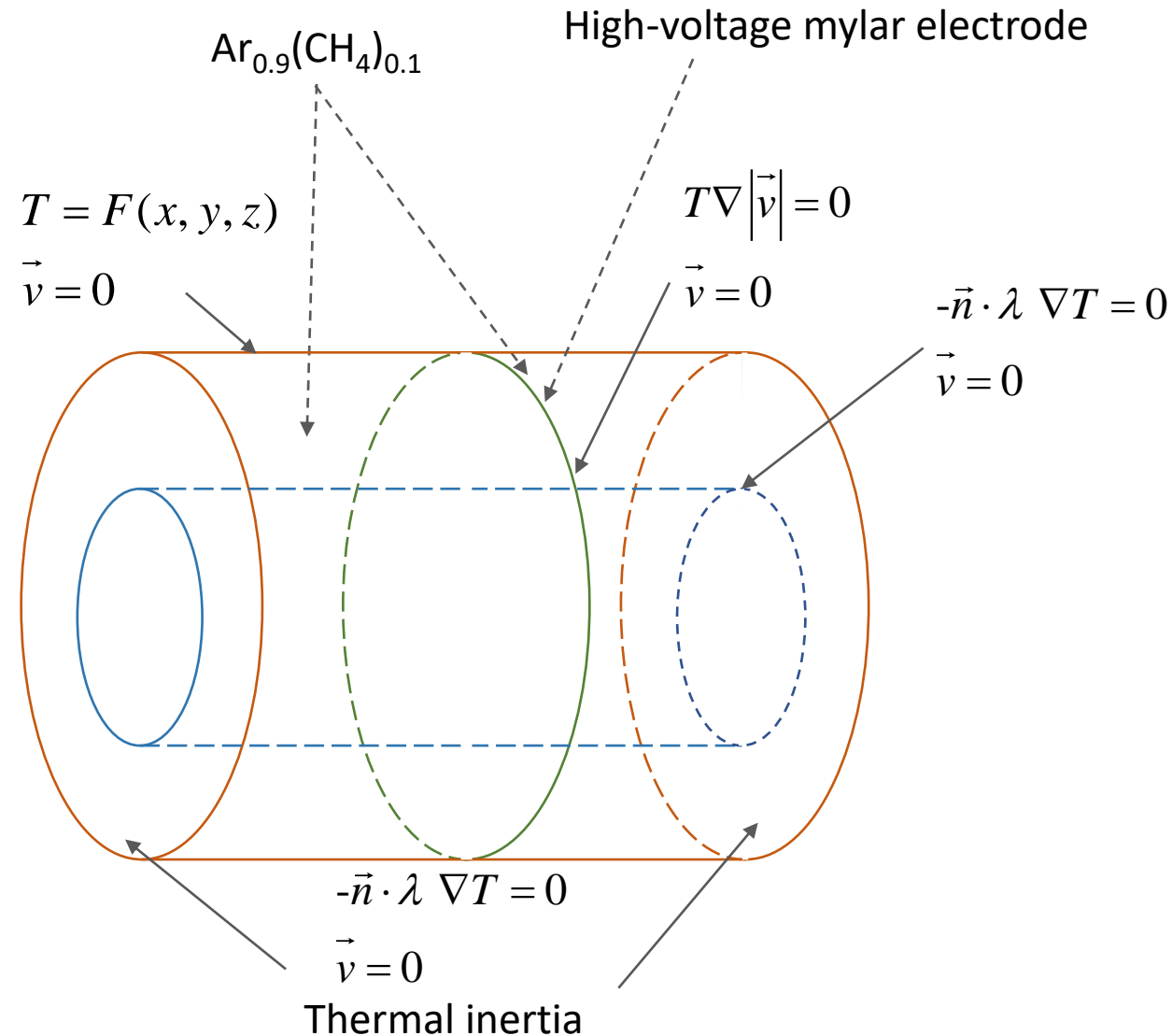
Screen is being heated from outside by Time-of-flight detector. Temperature spatial distribution is expected to be non-uniform due to **difference in adhesive thermal resistance** and **screen construction**

We consider possible temperature amplitude from 0.1 to 2.5 K

$$F(x, y, z) = T_a \cdot \sin\left(k_{long} \cdot \frac{\pi}{L_{gasTPC}} z\right) \cdot \sin(k_{rad} \cdot \arctg(y, x))$$



Temperature at gas volume boundaries



The model & the mesh

Navier-Stokes & heat transfer equation:

$$\begin{cases} \nabla \cdot \vec{u} = 0 \\ \rho_0 \frac{\partial \vec{u}}{\partial t} + \rho_0 (\vec{u} \cdot \nabla) \vec{u} = -\nabla (p + \mu_0 \cdot \nabla \vec{u}) + \rho_0 \beta (T_0) (T - T_0) \vec{g} \\ \rho_0 C_{p0} \left(\frac{\partial T}{\partial t} + (\vec{u} \cdot \nabla) T \right) = \nabla \cdot \lambda_0 \nabla T \end{cases}$$

\vec{u} – velocity;

ρ – density;

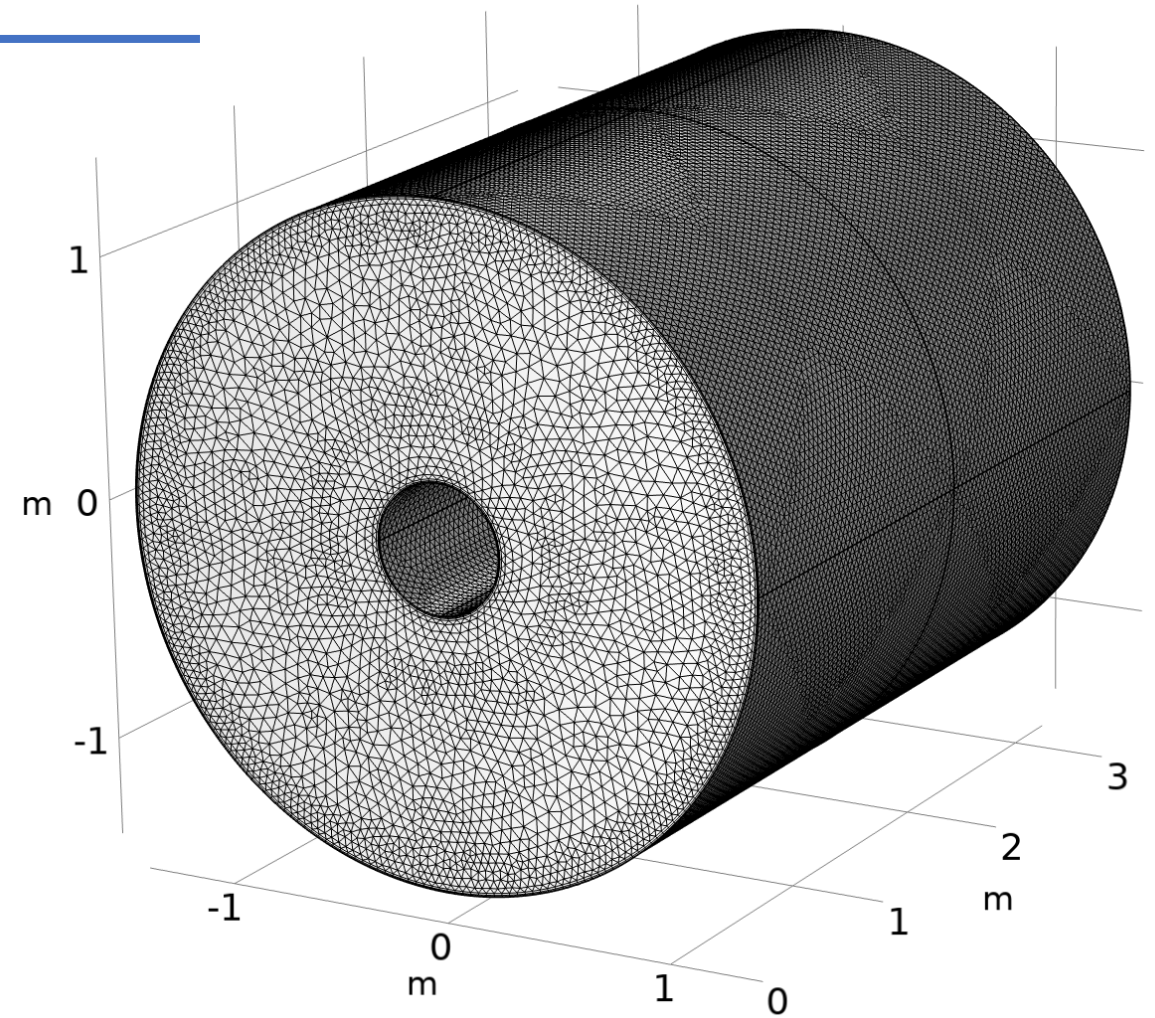
μ – dynamic viscosity;

p – pressure;

t – time;

λ_0 – heat transfer coefficient
at reference temperature T_0 ;

C_{p0} – heat capacity at reference
temperature T_0



Mesh resolution $\sim 2,2 \approx 10^6$ cells

Estimation of error

Kolmogorov's **scale η of smallest vortices** in isotropic turbulence can be defined as $\eta = \left(\frac{\nu^3}{\varepsilon} \right)^{\frac{1}{4}}$ where ν – kinematic viscosity, $\varepsilon \approx U'^3 / L$ is energy dissipation rate, where L – system length scale, U' – turbulent pulsating component of velocity (order of magnitude less than the average velocity).

For mesh step $h \approx 7$ cm and $\eta \approx 5$ cm we can compute a fraction of correctly resolved turbulent energy:

$$\delta_{E_{resolved}} = \frac{\int_{k_h}^{k_\eta} E(k) dk}{\int_{k_0}^{k_\eta} E(k) dk} = \left(\frac{k_h}{k_0} \right)^{-\frac{2}{3}} \approx 0.97, \quad \text{where } E(k) = C \varepsilon^{2/3} k^{-5/3} \text{ is Kolmogorov's spectrum.}$$

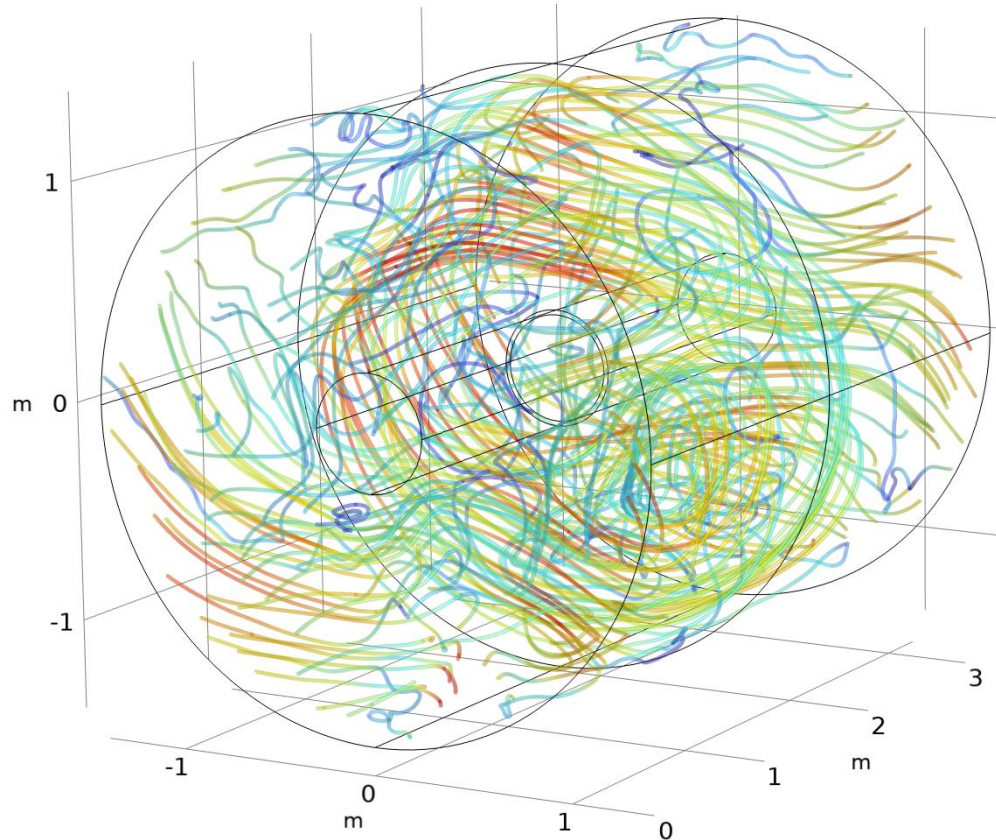
Wavenumbers are defined through lengths: $k_\eta = 2\pi / \eta$, $k_0 = 2\pi / L$, $k_h = 2\pi / h$

We expect 3 % of unresolved energy turbulent energy

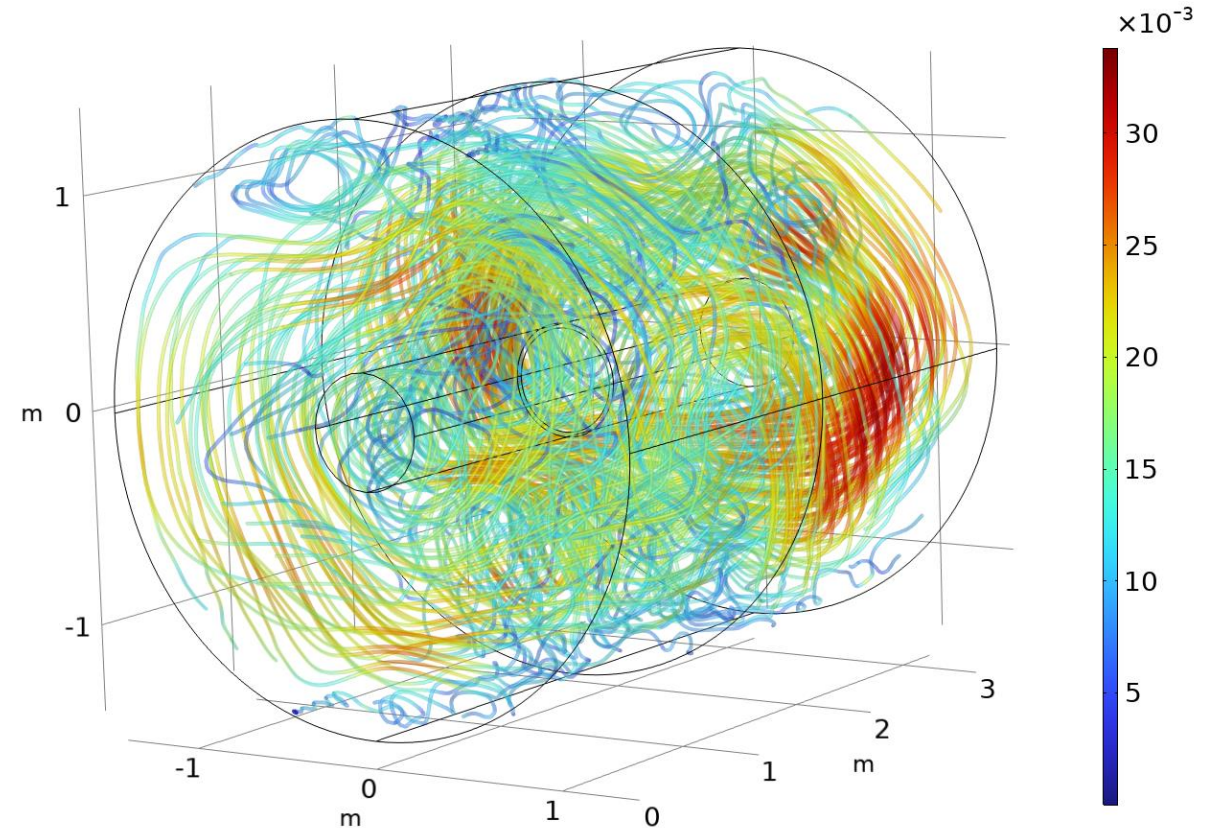
Instant streamlines

Instant streamlines, color scale – velocity (m/s), quasistationary state at $4 \cdot 10^4$ c

$\Delta T = 0.1$ K, $Ra \approx 2 \cdot 10^4$



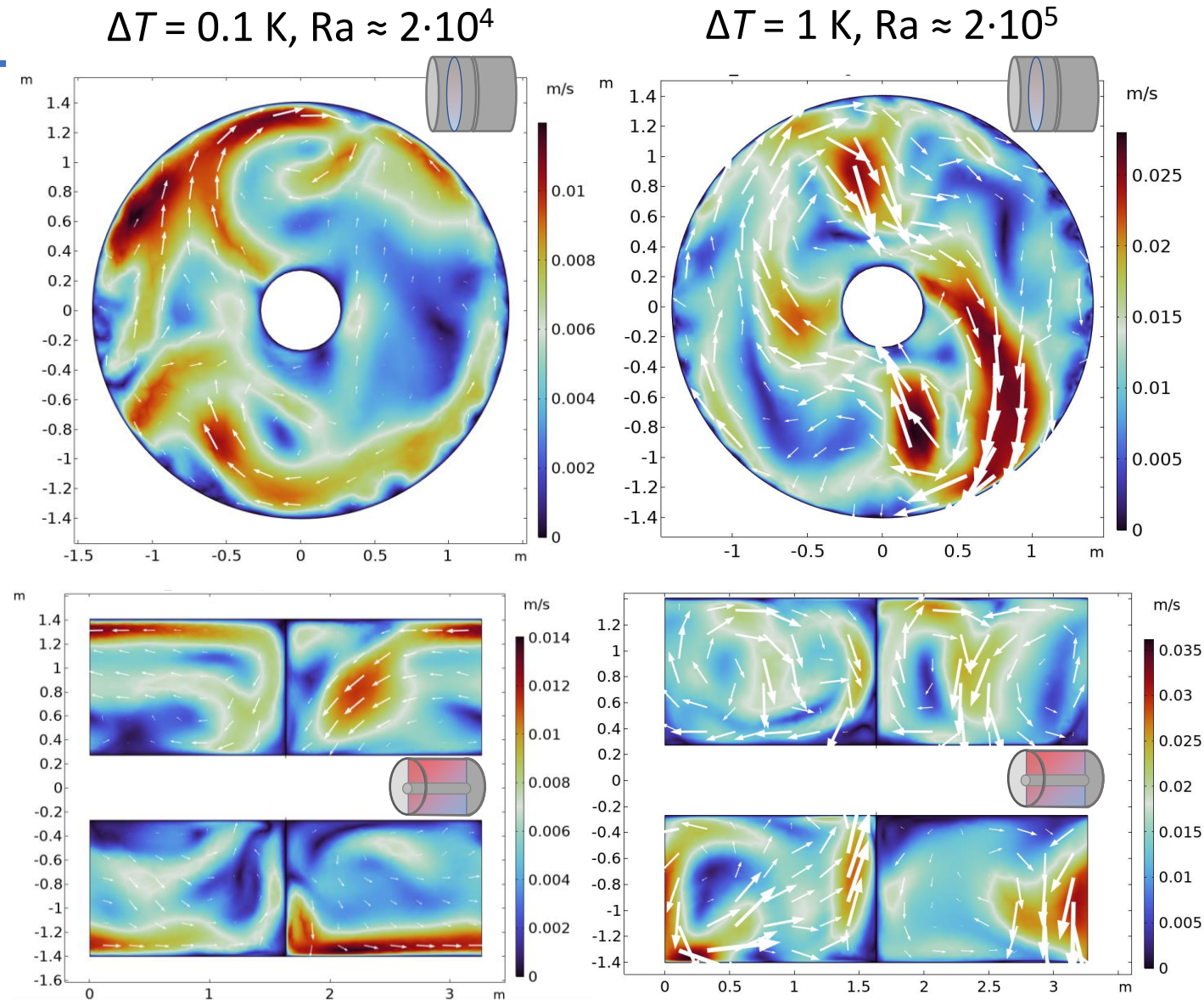
$\Delta T = 1$ K, $Ra \approx 2 \cdot 10^5$



Velocity slices

- For given temperature fluctuations gas velocity is about $(1 \div 5) \cdot 10^{-2}$ m/s;
- Highest velocity is at the boundaries of the computational domain;
- Quasi-stationary circulation is formed along the cylinder axis between the electrode and the TPC face.

Streamlines and velocity magnitude



Q-criterion & FTLE

Q-criterion – vortex search:

$$Q = \frac{1}{2} [|\Omega|^2 - |S|^2]$$

Difference between vorticity tensor norm

$$\Omega = \frac{1}{2} [\nabla \vec{v} - (\nabla \vec{v})^T]$$
 and viscous stress tensor norm

$$S = \frac{1}{2} [\nabla \vec{v} + (\nabla \vec{v})^T]$$

Finite-time Lyapunov Exponent – coherent Lagrange structures

$$\Lambda(\vec{r}, t_0, \Delta t) = \frac{1}{|\Delta t|} \ln \sqrt{\lambda_{\max} \left[\left(\nabla \phi_{t_0}^{t_0 + \Delta t}(\vec{r}) \right)^\top \nabla \phi_{t_0}^{t_0 + \Delta t}(\vec{r}) \right]}$$

where t_0 – initial time moment,

Δt – considered period of advection,

\vec{r} – coordinate vector,

λ_{\max} – maximum matrix eigenvalue operator,

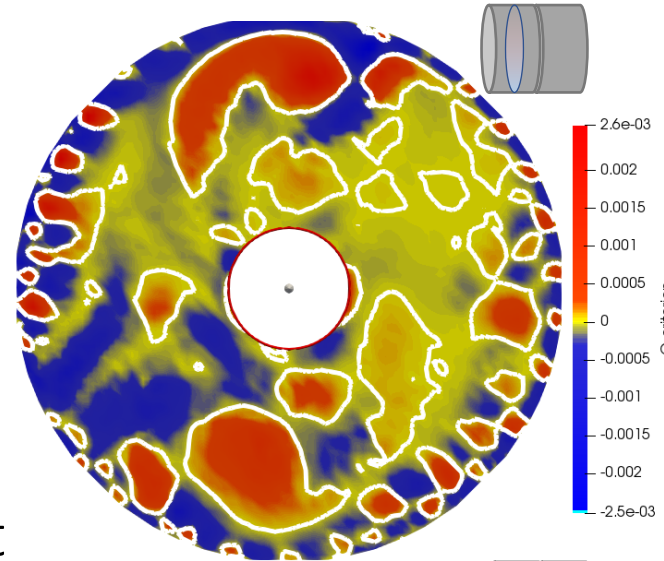
ϕ_{t_0} – flowmap, matrix operator mapping coordinates of

Lagrangian particle at time moment t_0 to coordinates at

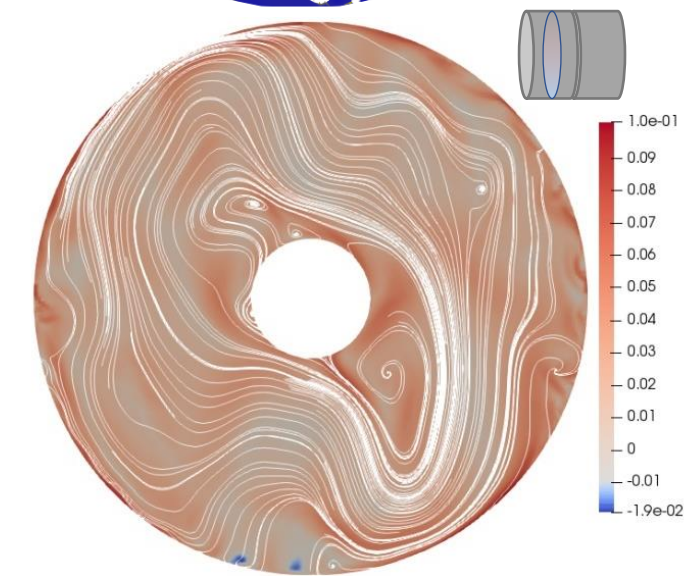
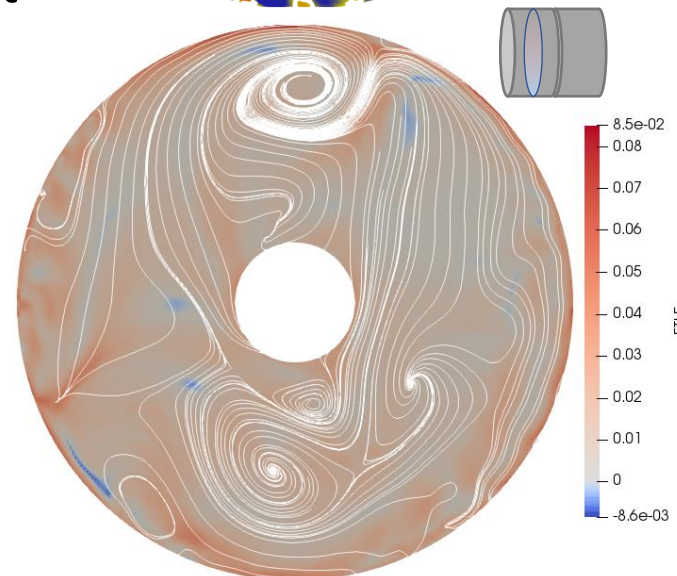
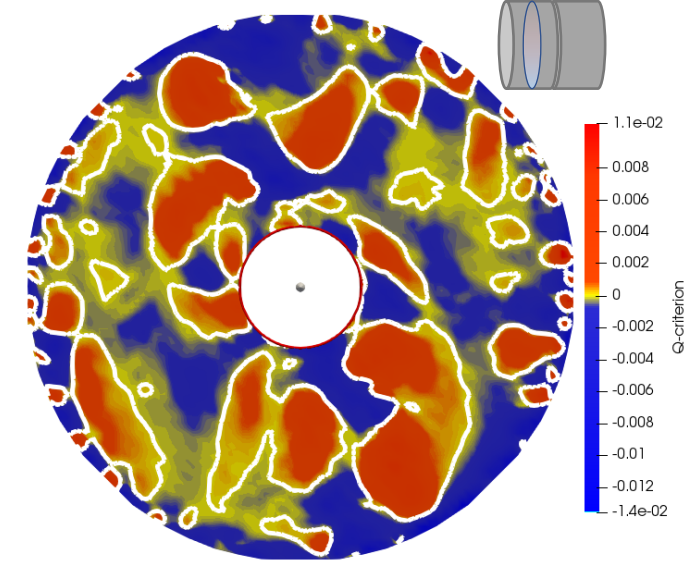
moment $t_0 + \Delta t$.

Q-criterion & FTLE

$\Delta T = 0.1 \text{ K}, Ra \approx 2 \cdot 10^4$

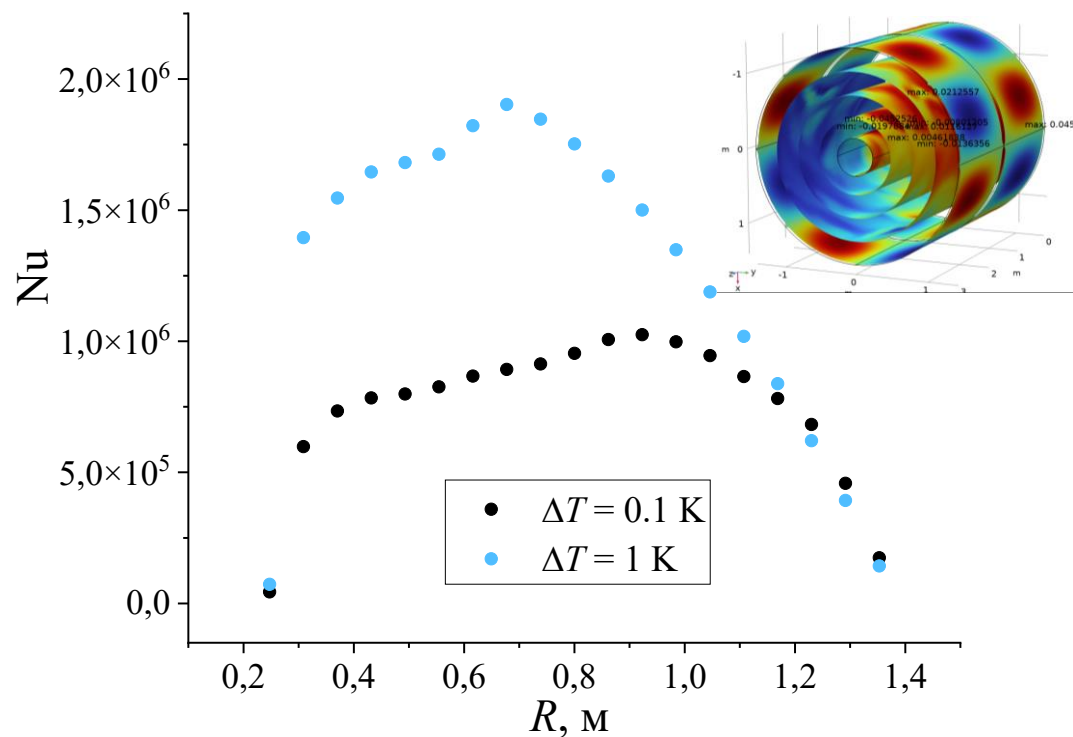


$\Delta T = 1 \text{ K}, Ra \approx 2 \cdot 10^5$

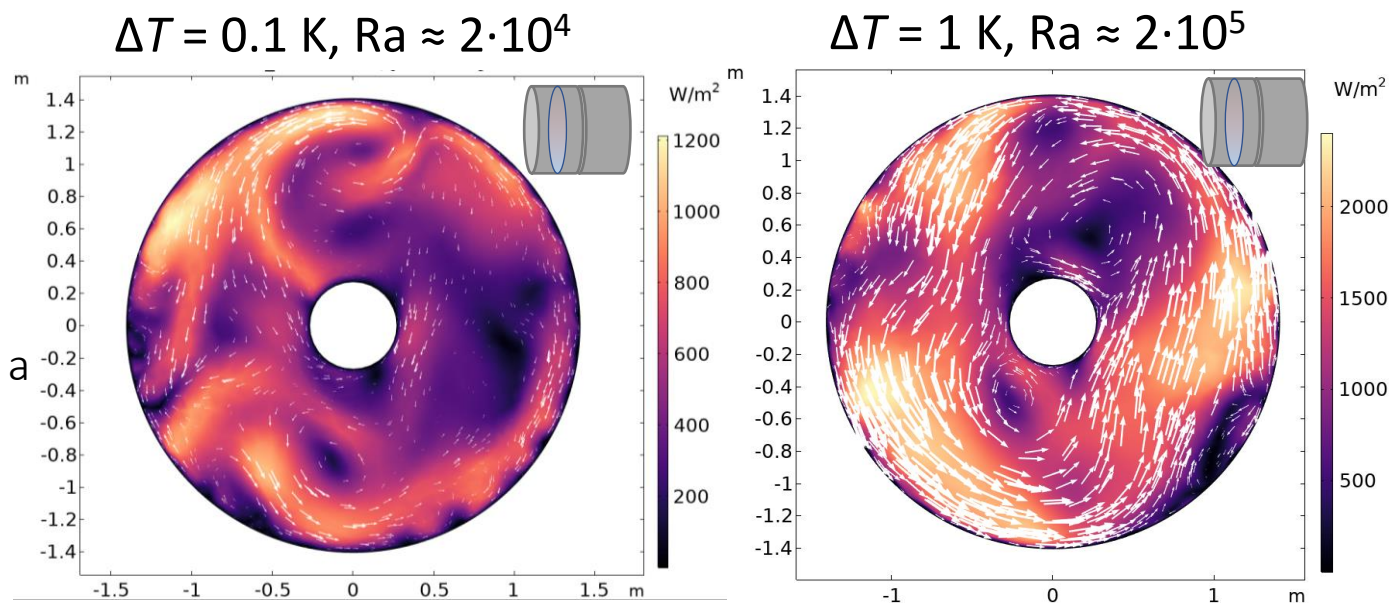


Temperature dynamics

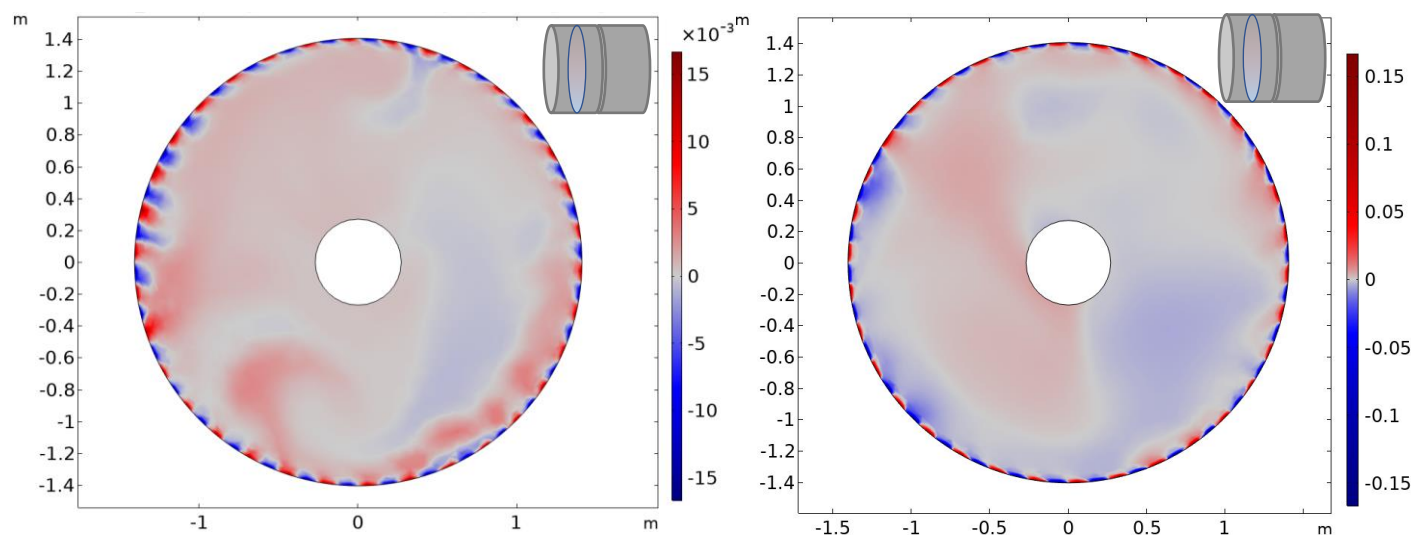
- Vortices occur between locally overheated and overcooled regions;
- The Nusselt number for all cases is 10^6 , decreasing at a distance of less than 0.2 metres from the walls



Heat flux



Temperature



Electronic drift

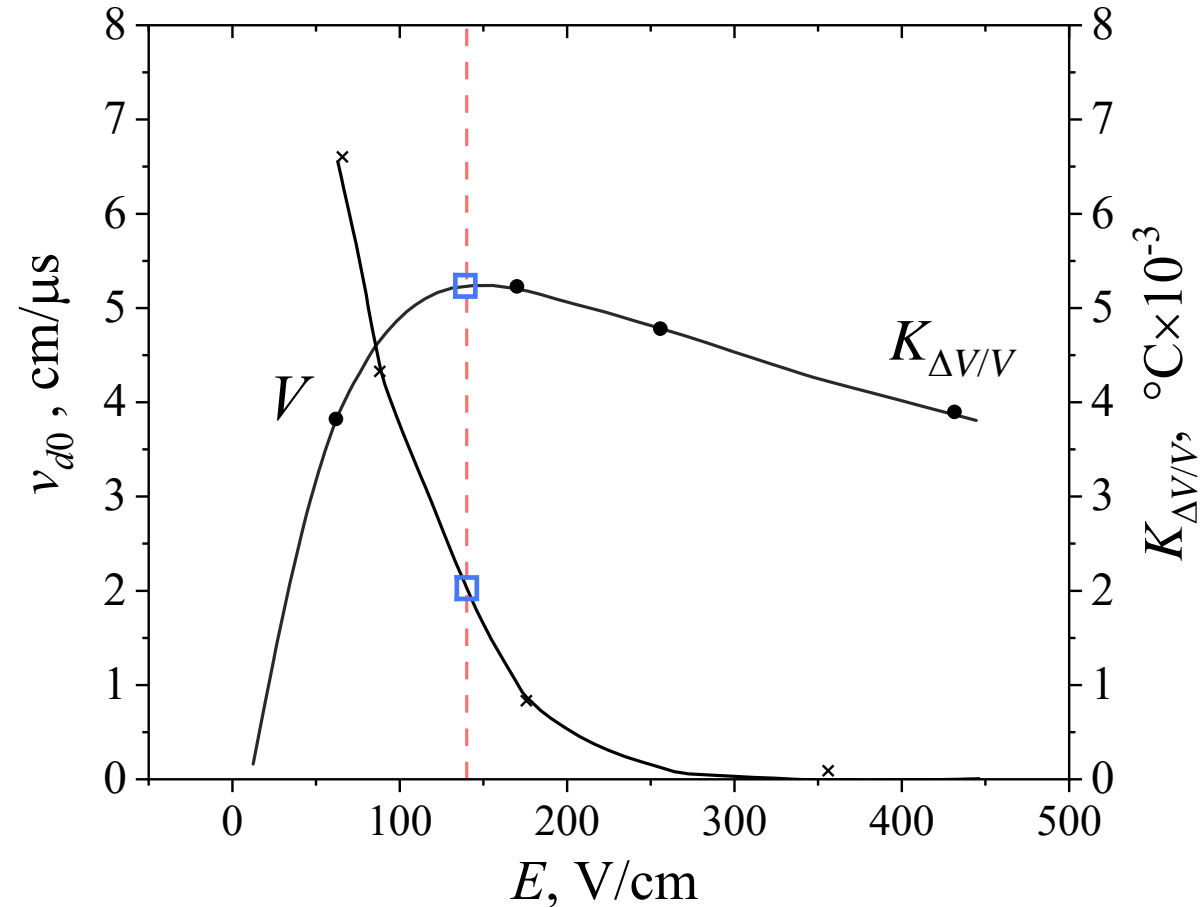
When beams collide, the highest yield of elementary particles is expected at sharp angle to the central electrode. The drift velocity \vec{v}_d of electrons to the ends depends on the local temperature $T(\vec{r})$:

$$\vec{v}_d = \vec{v}_{d0} + K_{\Delta V/V} \cdot \vec{v}_{d0} \cdot \theta$$

where \vec{v}_{d0} is drift velocity at thermal stabilization temperature,

θ – deviation from thermal stabilization temperature;

$K_{\Delta V/V}$ – coefficient of linear drift velocity change under electric field 140 V/m for given thermal stabilization temperature.



Field dependence of electron drift velocity and coefficient of linear drift velocity change in $\text{Ar}_{0.9}(\text{CH}_4)_{0.1}$ for 25 $^{\circ}\text{C}$

Peisert A., Sauli F. Drift and diffusion of electrons in gases: a compilation (with an introduction to the use of computing programs) // European organization for nuclear research. 1984. № July. P. 133.

Electronic drift

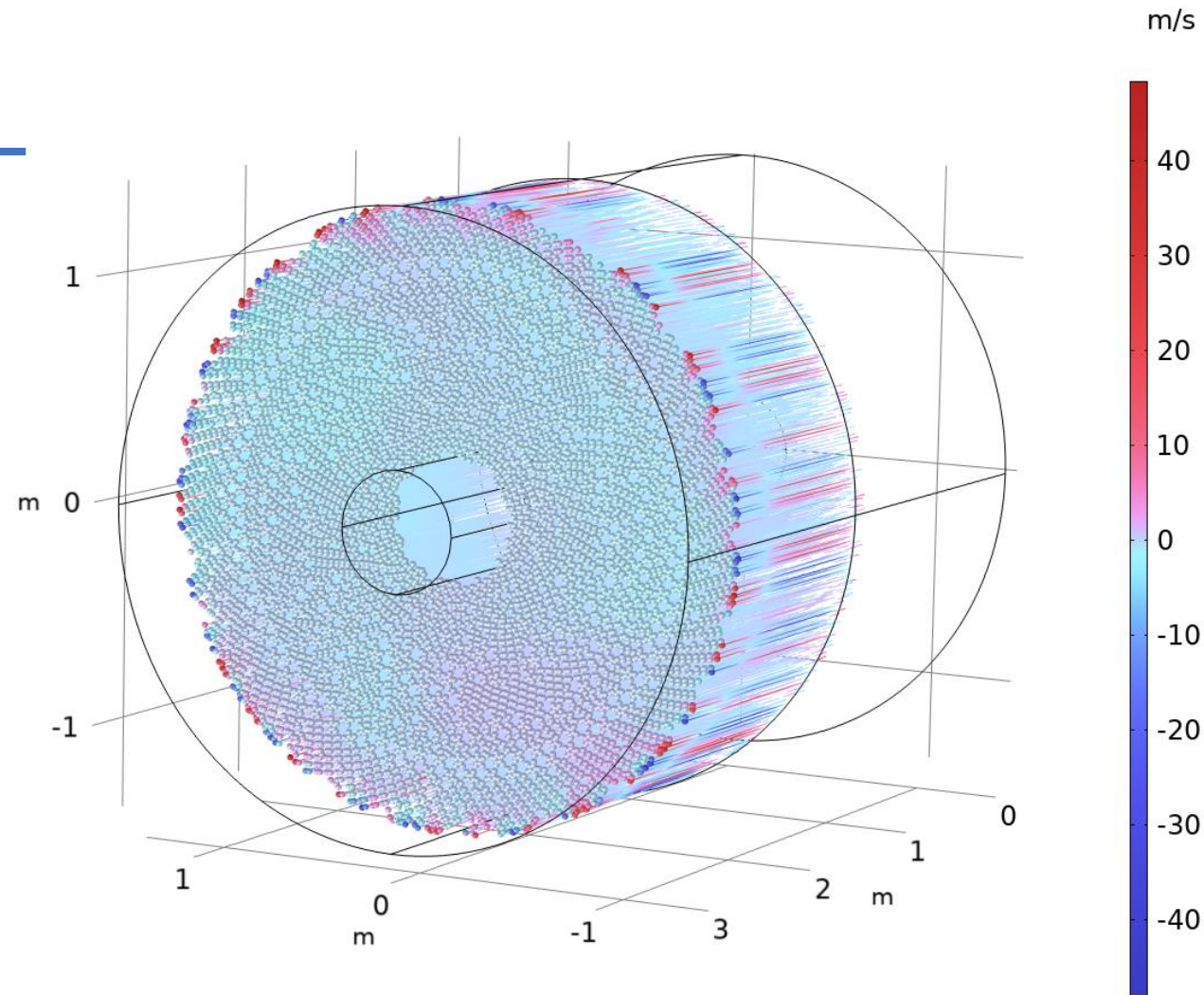
$dT=1$ K, Рой электронов (цвет - отклонение от скорости термостабилизации)

Cauchy problem for a single electron:

$$\begin{cases} \frac{d\vec{r}_e(t)}{dt} = \vec{v}_d(T(\vec{r}_e))dt \\ \vec{r}_e(0) = \vec{r}_{e0} \end{cases}$$

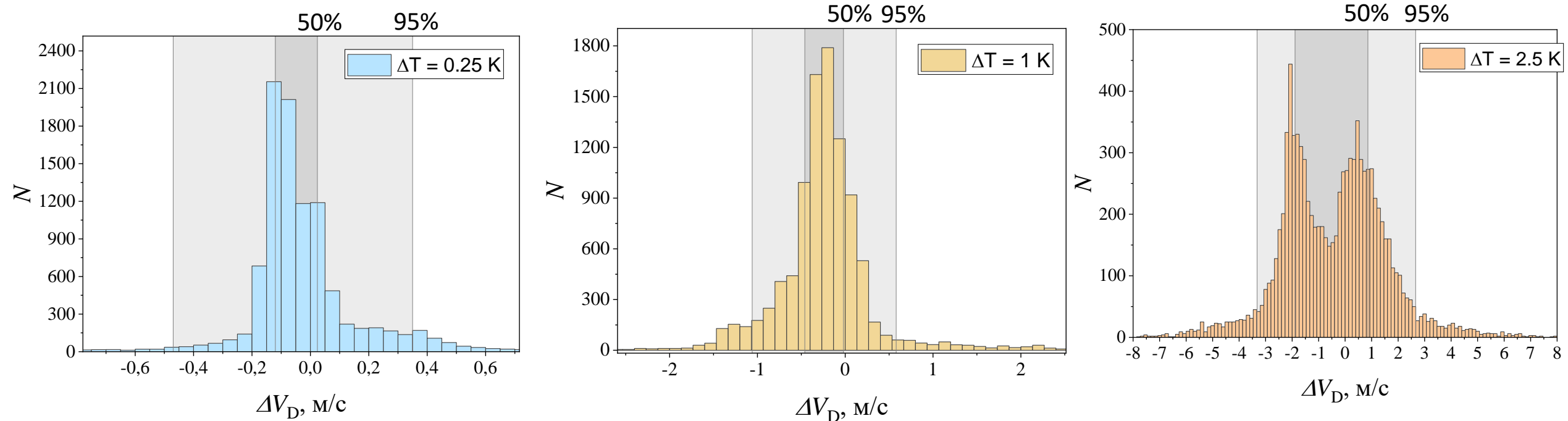
Algorithm:

1. Solution of the equations of gas dynamics and heat transfer;
2. Solution of the equations of electron motion from the track using the spatial distribution of temperature of the medium.
3. Analysis of statistical characteristics of electron drift.



Swarm of electrons drifting from the high-voltage electron to the end face of the working gas volume at the temperature fluctuation amplitude of 1 K

Electronic drift



Distribution of deviations from mean electron drift velocity for different amplitude of temperature fluctuation

ΔT , K	$\Delta V_{50\%}$, M/c	$\Delta V_{95\%}$, M/c	$\Delta t_{50\%}$, c	$\Delta t_{95\%}$, c	$\Delta x_{50\%}$, M	$\Delta x_{95\%}$, M
0.1	0.074	0.15	$3.4 \cdot 10^{-10}$	$6.1 \cdot 10^{-10}$	$6.0 \cdot 10^{-6}$	$1.2 \cdot 10^{-5}$
0.25	0.08	0.41	$2.9 \cdot 10^{-10}$	$1.7 \cdot 10^{-9}$	$6.5 \cdot 10^{-6}$	$3.3 \cdot 10^{-5}$
1	0.22	0.82	$8.9 \cdot 10^{-9}$	$3.3 \cdot 10^{-9}$	$1.7 \cdot 10^{-5}$	$6.6 \cdot 10^{-5}$
2.5	1.38	2.99	$5.6 \cdot 10^{-9}$	$1.2 \cdot 10^{-8}$	$1.1 \cdot 10^{-4}$	$2.4 \cdot 10^{-4}$

Conclusions

- A model of heat transfer in the working gas volume of the MPD unit of the NICA accelerator complex has been developed, the corresponding initial boundary value problem has been solved by the finite element method;
- The following features of the flow were found:
 - a. heat transfer occurs primarily due to convective which is supported by $Nu \sim 10^6$;
 - b. appearance of flows carrying heated and cooled gas deep into the working volume occurs due to the rotation of small vortices at the boundaries caused by temperature differences at the boundaries;
 - c. temperature deviation of $Ar_{0.9}(CH_4)_{0.1}$ from the thermal stabilisation temperature monotonically decreases when moving away from the outer boundary of the gas volume, reaching to the centre of the working volume not more than 0.01 K;
- A method is proposed and implemented for the calculation of the drift velocity of the electron swarm in the working gas volume from the solution of the equations of motion, taking into account the dependence of the drift velocity on the local gas temperature;
- It was found that 95% of electrons have an error of no more than $7 \cdot 10^1 \mu m$ in restoring the initial coordinate at temperature difference amplitudes of 1 K at the boundary.

The boundary conditions will be refined to account for heat generation on the ToF, and the calculations will be refined using the Nek5000 code on the supercomputer

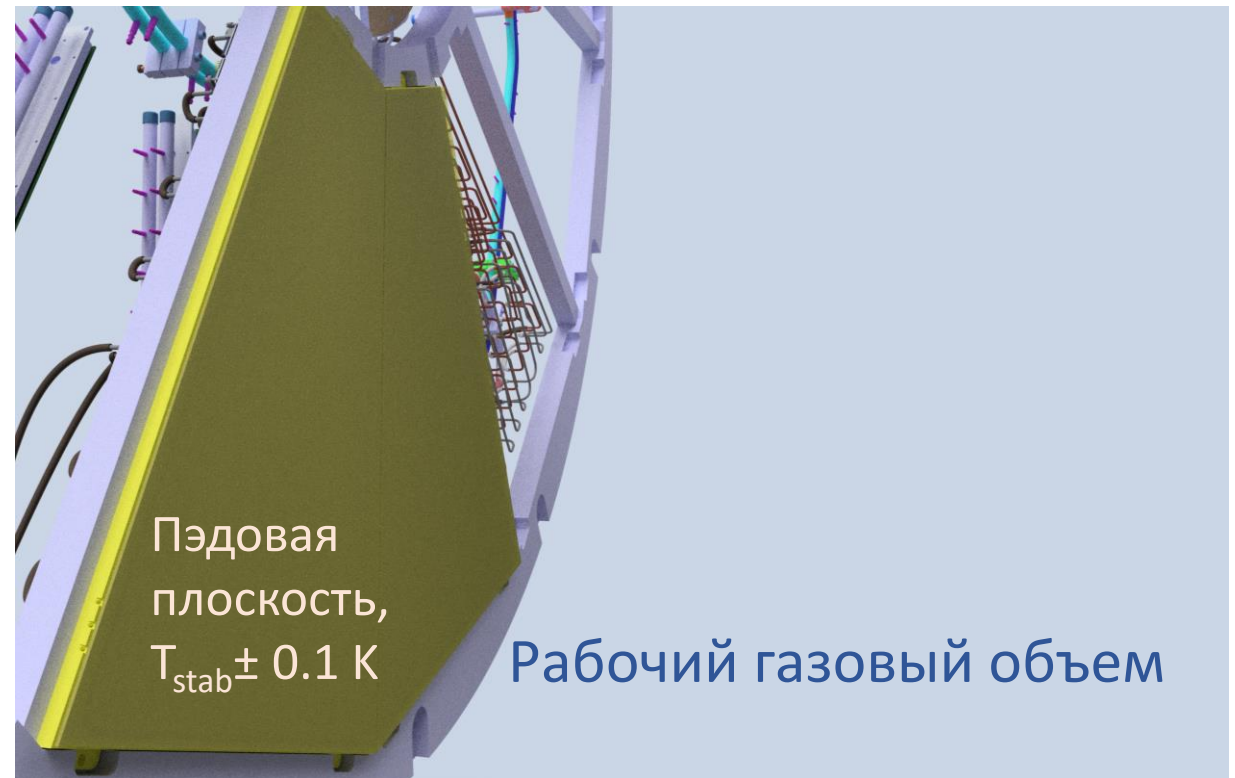
Thank you for your attention

Допслайды

Разработка экспериментальных устройств

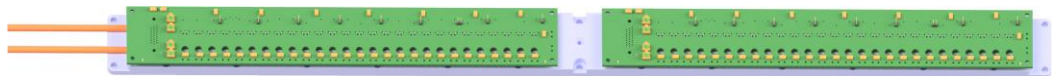
Для запуска MPD **достаточна термостабилизация 1 К**, но для развития комплекса понадобится замена газа и термостабилизация **до 0,1 К**

- Необходимы датчики температуры высокой точности;
- Нужна система подготовки термостабилизированного газа;
- Понимание, возможен ли такой режим в принципе

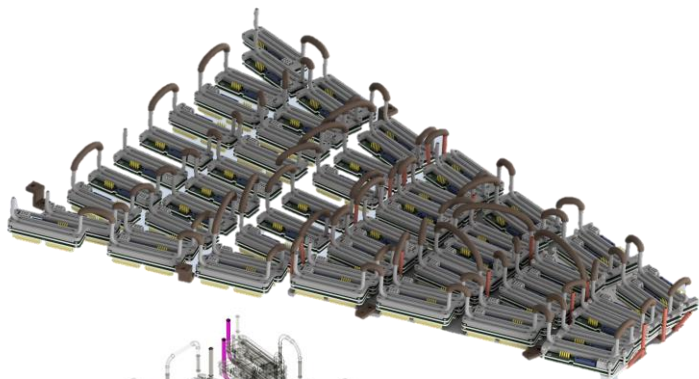


Пэдовая плоскость контактирует с торцом газового объема

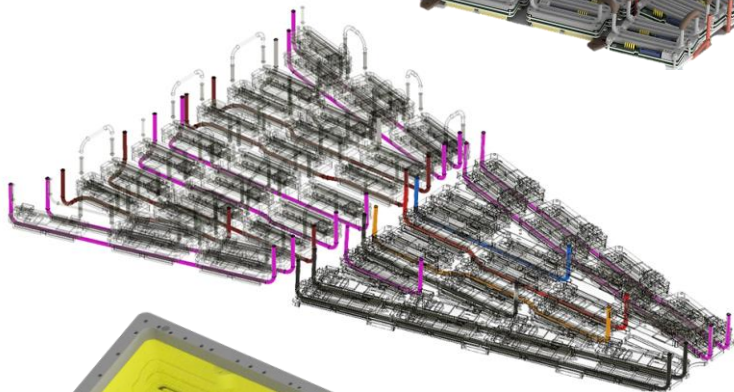
Связанная система ROC



LVDB



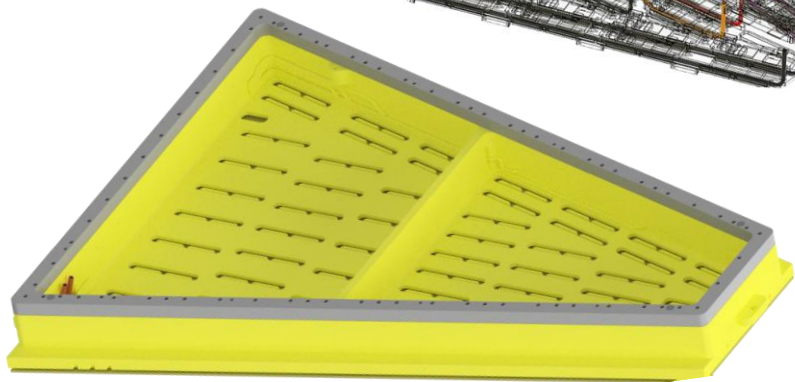
FPGA



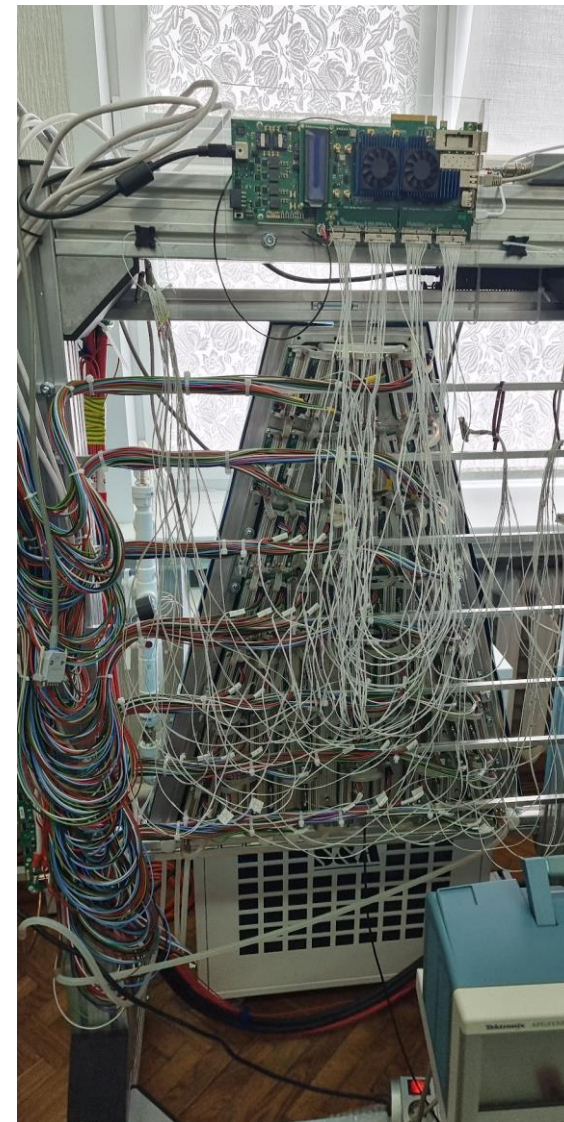
SAMPA



ROC case



Water supply



Electric cables

Проверка термостабилизации плоскости ROC

Эксперимент:

- Вода подается **4** **раздельными линиями**;
- **Камера электроники ROC** **теплоизолирована** **от** **окружения**;
- Комната кондиционирована;
- Тепловизор находится в темноте и калиброван по контактными датчикам температуры.

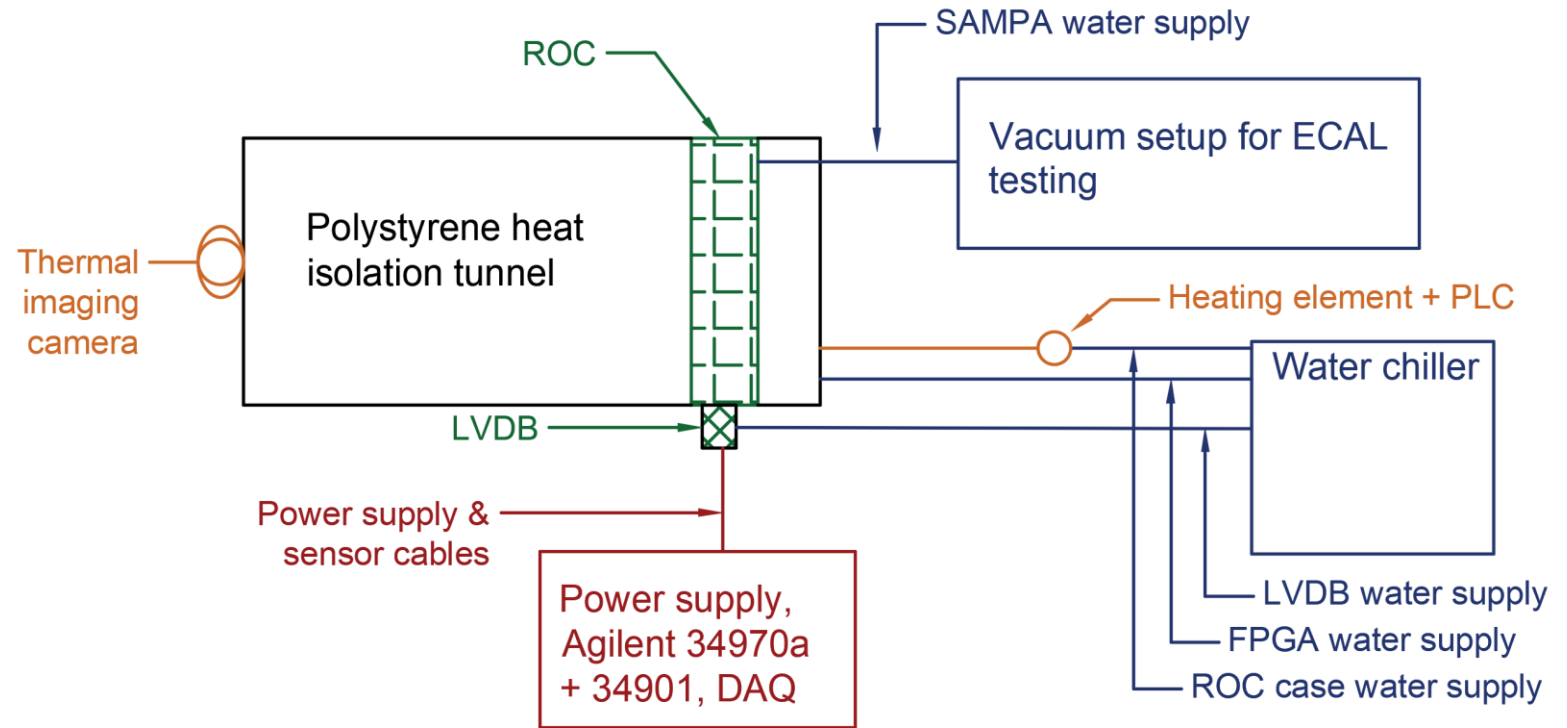
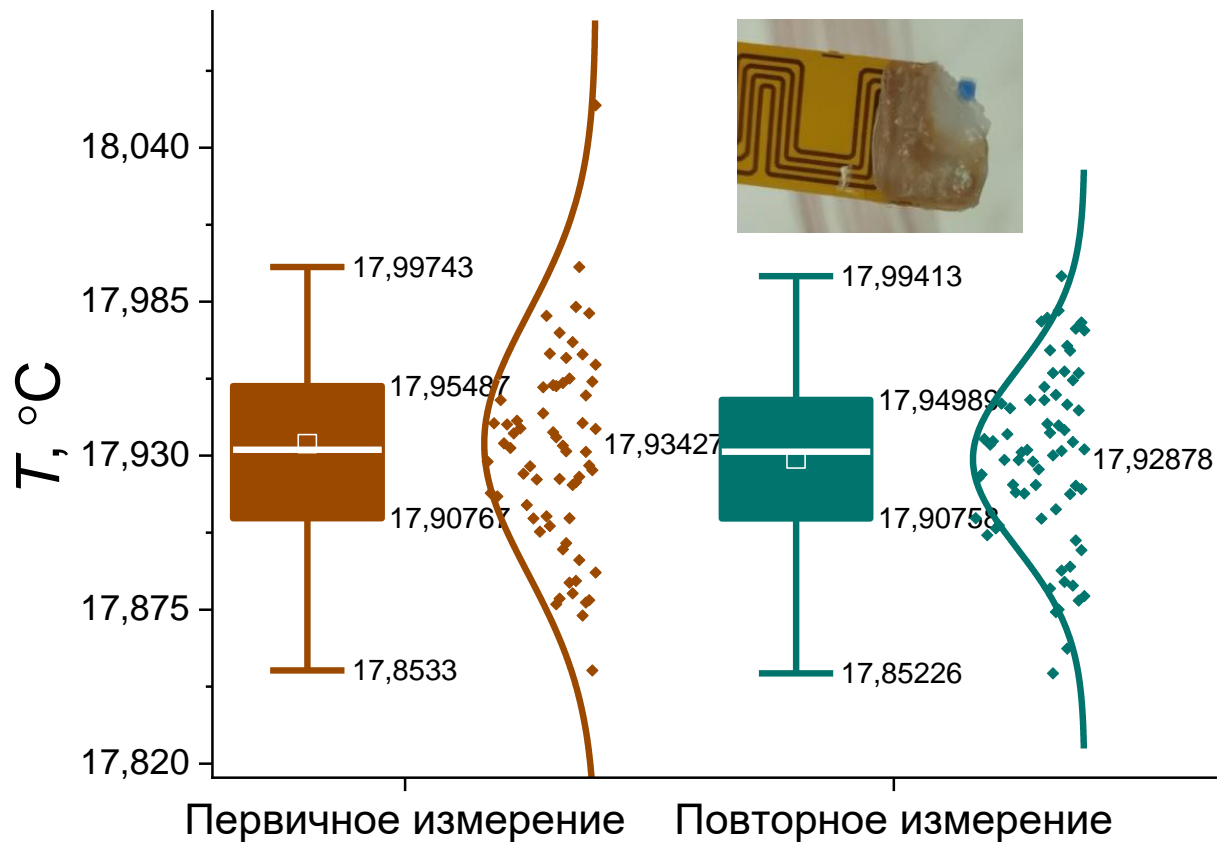


Схема эксперимента

Используемые датчики

С точностью 0,01 К датчики Pt100 в России не сертифицируют, проведена калибровка с помощью Элемер-ТК-М150-К

https://youtu.be/_kcda9WyVOU



https://rutube.ru/video/private/fc768c02ae8ce14493c1f14abc95949b/?p=MdkkueBE9O_rzah2Bd1gRA&r=plwd

Выбирались датчики из коридора ± 0.02 К от среднего

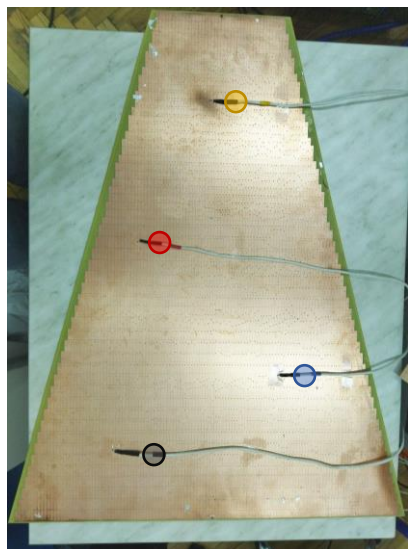
Экспериментальная установка

Степень термостабилизации

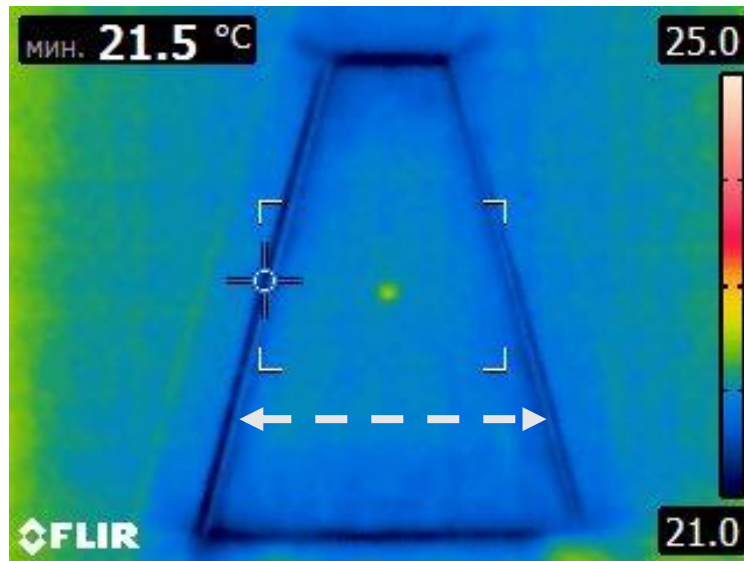
Внешний воздух: 24°C

SAMPA вода на входе: 25°C (стационарно)

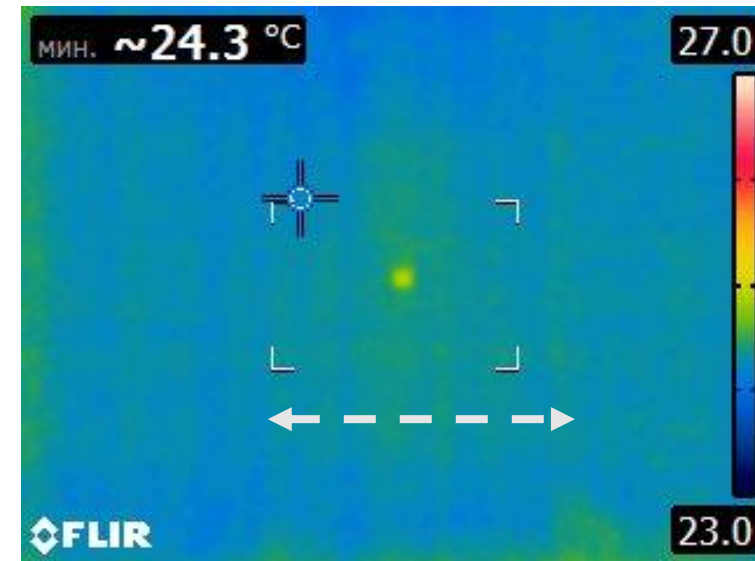
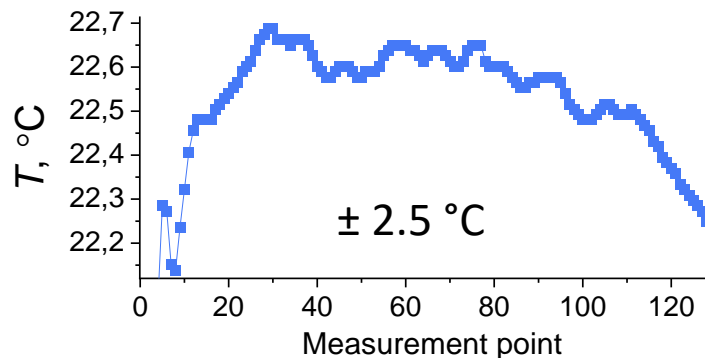
FPGA вода на входе: 17-18 °C



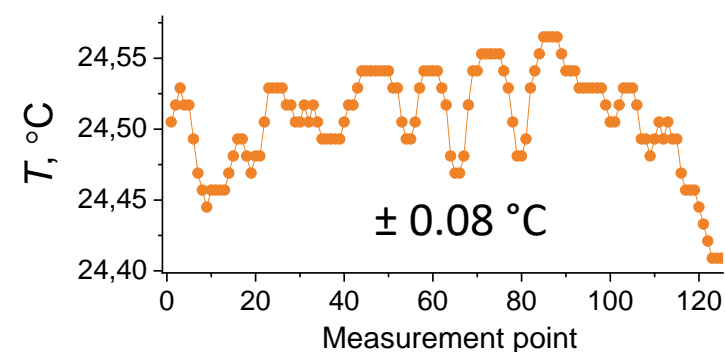
Тепловизор Flir E8 был калиброван отобранным и Pt-100 терморезисторами



Пэддовая плоскость без адаптивной температуры в контуре корпуса ROC



Вода в корпусе ROC догревается до $T = 23\text{ °C}$



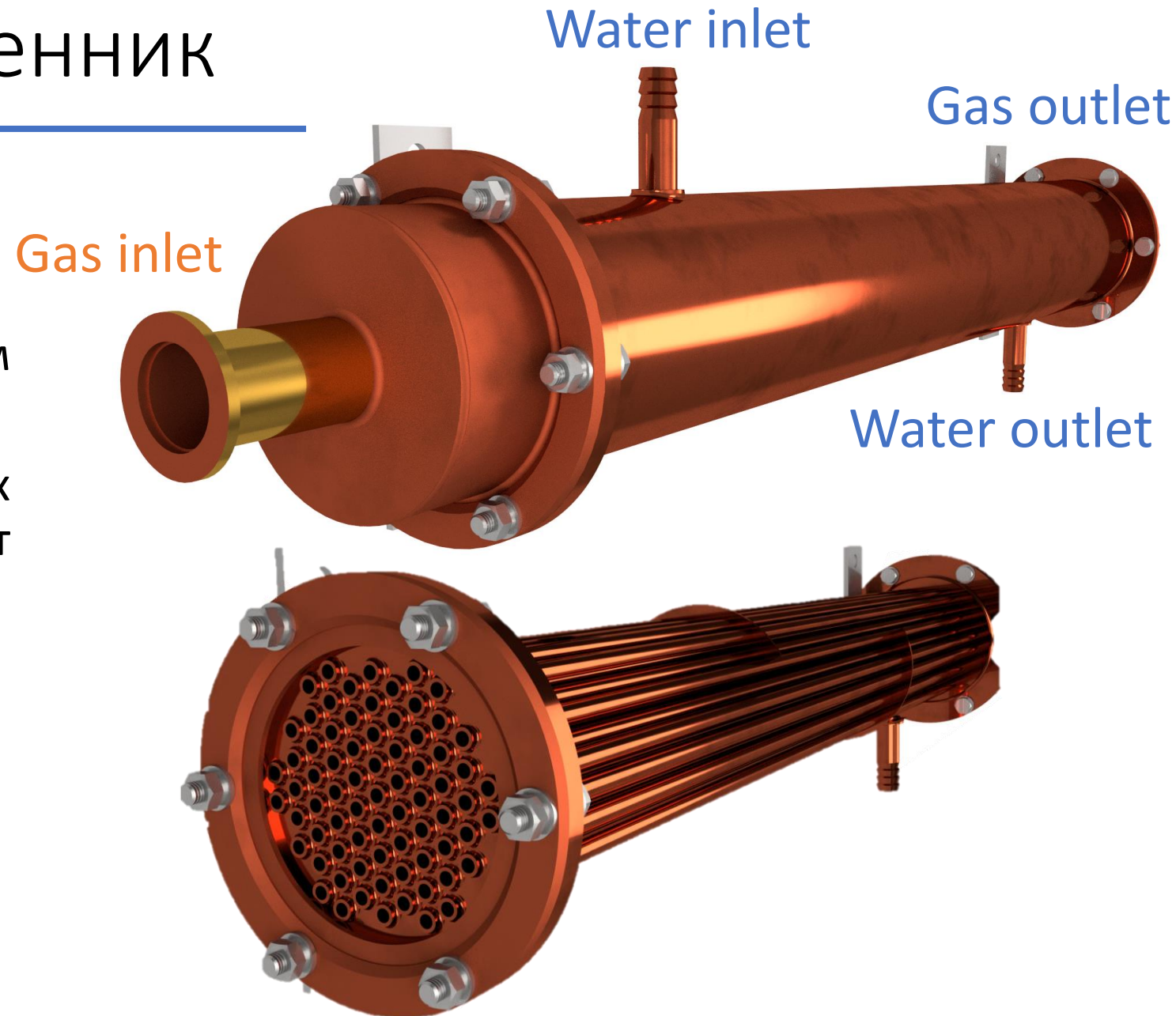
Сенсор	$T_{\text{sensor}}, \text{ °C}$	$T_{\text{camera}}, \text{ °C}$
Желтый	21,82	21,87
Красный	21,67	21,67
Синий	21,50	21,56
Серый	21,86	21,87

Газовый теплообменник

Кожухотрубный теплообменник:

- Газ течет по 74 малым трубкам диаметра 6 мм;
- **Водяной слой** снаружи малых трубок обеспечивает теплообмен;
- Вес 8 кг

В процессе изготовления

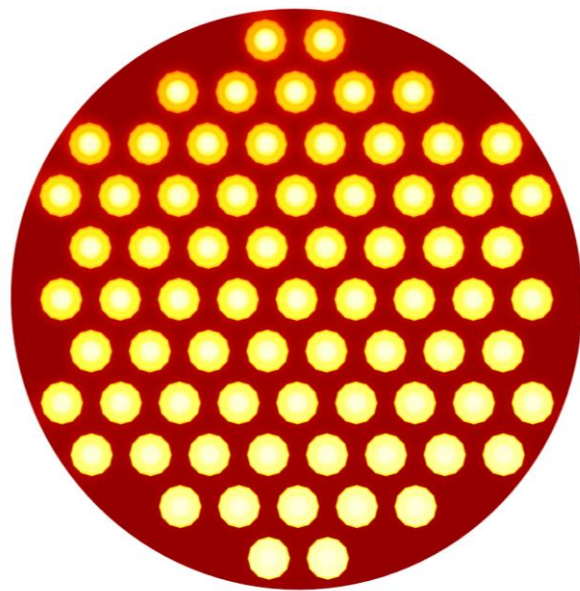


Газовый теплообменник

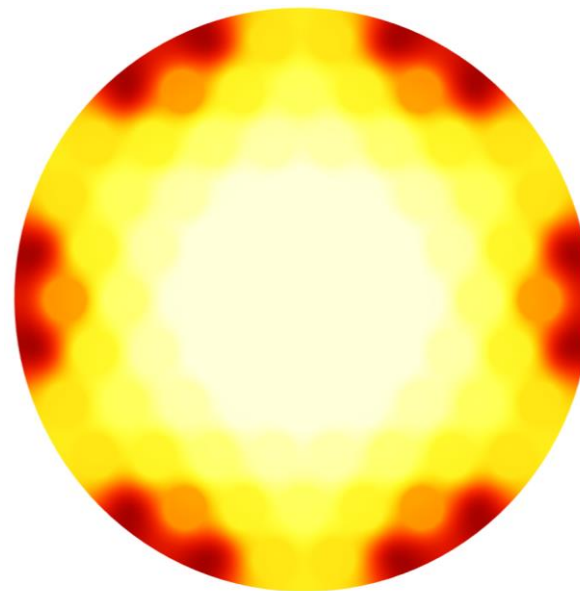
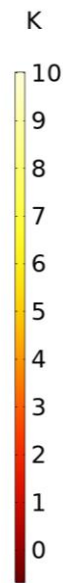
Prototype simulation parameters:

- Length 0.55 meters;
- Inlet gas is 10 K hotter than water;
- Water flow is 0.1 m³/h;
- Gas flow is 20 — 200 l/min.

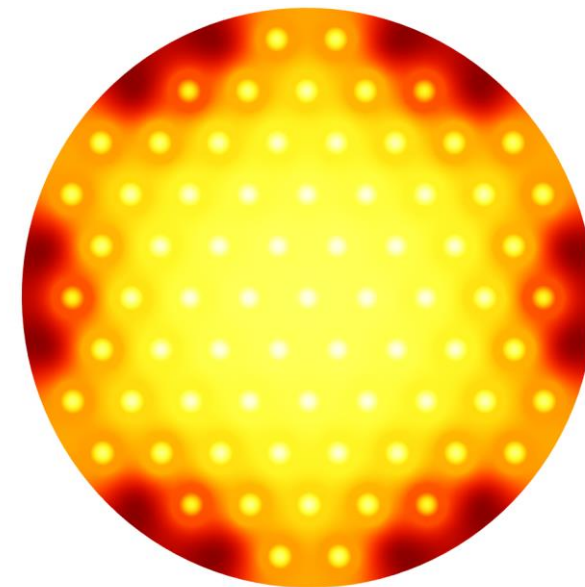
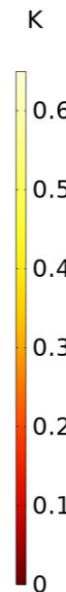
ΔT decreased by 10 times



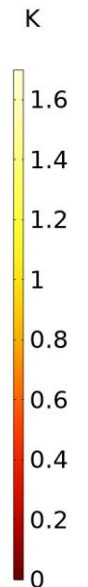
At inlet



At outlet – 20 l/min



At outlet – 200 l/min



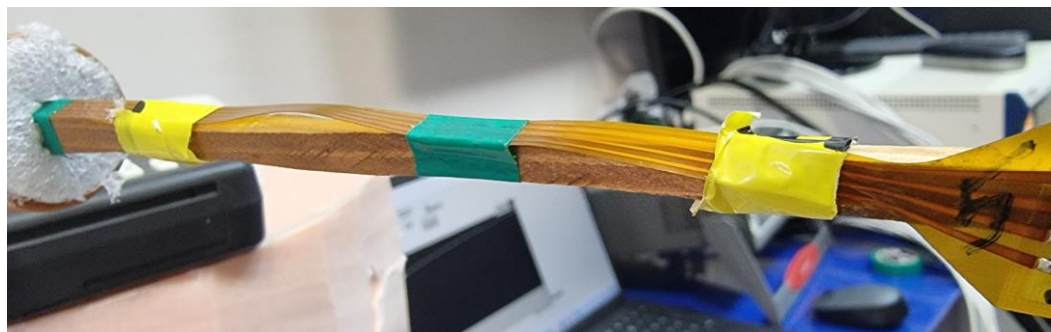
Gas temperature sensor

Experiment was motivated by Gleb Meshcheryakov

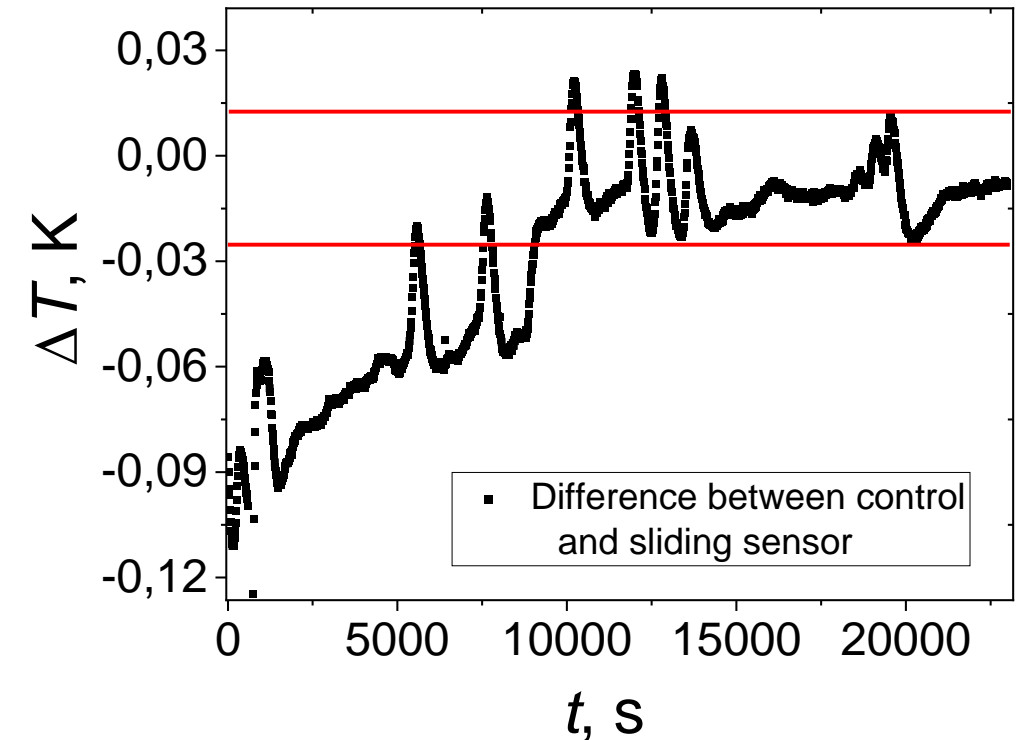
- Argon flow $\approx 800 \text{ cm}^3/\text{min}$;
- Water jacket is around testing tube;
- Pt100 RT + NI Controller;



Testing tube with sensor fully in



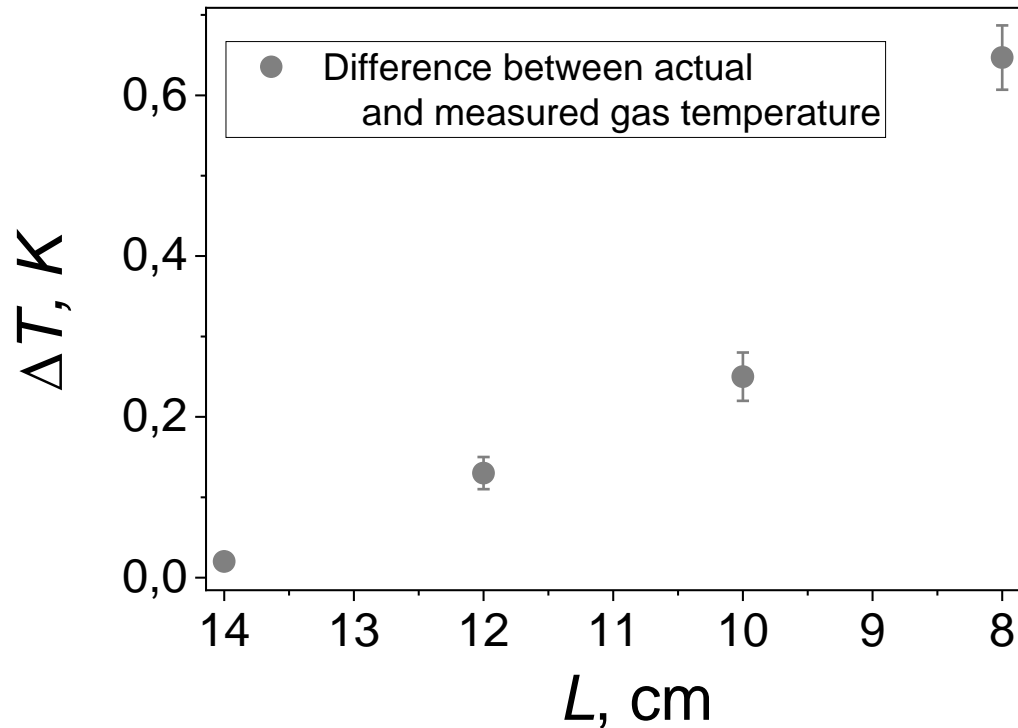
Sliding sensor almost out of tube



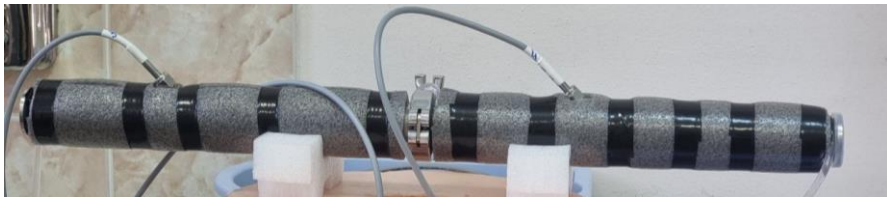
Time dependence of ΔT between the control and the full-drawn sliding sensor

$<0.03 \text{ K}$ gradient is achieved inside the testing tube with gas about $15 \text{ }^\circ\text{C}$ and room temperature $21 \text{ }^\circ\text{C}$

Gas temperature sensor



Difference between control and sliding sensor temperature on the length of wires inside gas



Prototype of gas temperature sensors with swagelok and wire support

Выводы по экспериментальной части

- **Prototypes of temperature sensors** for the flowing gas have been proposed and manufactured, with an expected measurement accuracy of 0.03 K;
- **Functioning front-end electronics** of the ROC was stabilized using four water lines equipped with ultrasonic flowmeters and controlled via programmable logic controllers. The temperature uniformity achieved on the pad plane was not worse than 0.1 K, which meets the requirements for MPD experiments.